



Influence of Uncertainty in the Elastic Modulus of Soil on the Combined Axial and Laterally Loaded Pile Group

Saikumar Kotra¹ · Kaustav Chatterjee¹

Received: 1 January 2024 / Accepted: 7 March 2024
© The Author(s), under exclusive licence to Indian Geotechnical Society 2024

Abstract Pile foundations generally experience various combinations of lateral and vertical load components i.e., axial and lateral loads. The present finite-difference study examines the static response of the pile group subjected to the combined vertical and lateral loads in the cohesionless soil. The soil is considered as a Mohr–Coulomb constitutive material, the pile material as linearly elastic material and the pile cap as a shell element in this study. A 2×2 pile group embedded in the cohesionless soil is considered in the study. The behaviour of the pile group relates to the properties of soil medium, especially the friction angle and the elastic modulus. It is well known that the soil, being the natural material, comprises uncertainties in its parameters. The parameter uncertainty i.e., the variation of the soil property is incorporated with the use of lognormal probability distribution pertaining to the parameter's coefficient of variation. The elastic modulus of the soil is considered for the inclusion of parameter uncertainty in the present three-dimensional study. The aim of the study is to investigate the lateral deflection, bending moment of pile group under the simultaneous action of axial and lateral loads. The incurring soil reaction due to the lateral resistance of piles when the lateral load is applied is also determined, envisaging the importance to study the p - y curves at various depths. The statistical variation in the form of probability density function and cumulative density function of the pile bending moments and lateral deflections are evaluated. The

numerical responses indicate that the parameter uncertainty of the soil properties and their coefficient of variation play a substantial role in the depiction of magnitudes of bending moment and lateral deflection.

Keywords Pile foundations · Finite-difference · Parameter uncertainty · Elastic modulus · Coefficient of variation · p - y curves

Abbreviations

COV	Coefficient of variation
f_i^l	Damping force
F_i^l	Out-of-balance force of the node
v_i	Grid point velocity of the node
M	Mass of the node
σ_{ij}	Stress tensor
b_i	Body force
ρ	Mass density
Δe_{ij}	Strain increment
H_{ij}^*	Incremental parameter in constitutive formulation
k	Loading history parameter
k_n	Normal stiffness
k_s	Shear stiffness
L	Length of pile
D	Diameter of pile
Q	Lateral load on the pile group
V	Axial or vertical allowable load on the pile group

✉ Saikumar Kotra
saikumar.iitr@gmail.com; ksaikumar@ce.iitr.ac.in
Kaustav Chatterjee
kaustav.chatterjee@ce.iitr.ac.in

¹ Department of Civil Engineering, Indian Institute of Technology Roorkee, Roorkee 247667, India

Introduction

Pile foundations are more often laid for the high-rise or massive civil structures, when the existing soil medium is weak and vulnerable to large degree of settlements. Pile foundations are generally classified as single and groups; wherein

the constructions utilize pile groups in common. Pile foundations usually support the lateral and vertical loads, and in few situations, piles are laid to support the combination of both. Even so, the behaviour of the pile groups under such load conditions is assessed individually, and the combined axial and lateral load behaviour is seldom investigated. This approach may lead to an improper design, seeing that most of the structures are subjected to coexisting axial and lateral loadings. In such case of load combination, it is also essential to study the possible interaction effects that occur inwardly.

To date, many researchers investigated the pile groups' behaviour when subjected to axial and lateral loads experimentally [1, 2]; analytically and numerically utilizing the finite-element or the finite-difference methods [3–9]. Anagnostopoulos and Georgiadis [10], based on the experimental model tests and the two-dimensional finite element analyses observed significant changes in the local plastic volume in the surrounding soil continuum when subjected to the combined axial and lateral loads. And so, they have recommended using a three-dimensional finite element or finite difference methodology for investigating the pile group problem.

Achmus and Thieken [11] studied the pile group behaviour in cohesionless soil when subjected to combined action of axial and lateral loadings. Authors stated that the combined load incurs the interaction effects by the virtue of the concurrent generation of passive earth pressure due to presence of lateral loads and the pile skin friction due to the application of axial loads. Karthigeyan et al. [12] reported that the lateral load capacity was increased due to the action of axial loads in cohesionless soil. Hussien et al. [13, 14] studied the interaction behaviour of pile groups subjected to axial loads, using the finite element method and found the minimal rise in lateral capacity of piles embedded in sand. Hazzar et al. [15] numerically evaluated the influence of vertical loads on the lateral performance based on 3D finite-difference analyses. Though there are research studies focusing the pile group behaviour when the axial load or lateral load is applied, but the numerical works that devote to the simultaneous axial or lateral load and the incurring soil reaction are seldom available.

Soil is a naturally formed geological material and it constitutes uncertainty due to its transportation and deposition and so, it accounts more uncertainty in comparison with the other engineering fields. Uncertainty lies with the majority of the soil parameters utilized in geotechnical studies. Ergo, it is inevitable to consider the uncertainty as one of the essential aspects of geotechnical analyses—the magnitude of uncertainty is proportional to its criticality and hence the need for its assessment on the influencing results. The major categorization of uncertainties in geotechnical engineering is aleatory and epistemic uncertainties. Aleatory uncertainty

relates to the inherent randomness of a property whereas, the epistemic uncertainty arises because of insufficient information pertaining to a property. Epistemic uncertainty relates to the measurement uncertainty due to instrumental and methodological imperfections, statistical uncertainty arising because of limited information and observations and the model uncertainty arising because of idealizations considered in the formulation of a geotechnical problem [16].

The uncertainty in the soil properties, viz., parameter uncertainty and the model uncertainty can be best assessed as random variables characterized by probability distribution function, their corresponding mean and standard deviation [16]. The normal and lognormal probability distributive functions are typically applied in the geotechnical analyses. The lognormal distribution is customarily utilized to represent the parameters that are non-negative in nature [17–19]. In most of the geotechnical studies, parameter uncertainty is characterized with the mean and coefficient of variation (COV). The ratio between the mean and standard deviation is termed as COV. With the notable number of soil parameters or the properties inclusive in the pile group study [20], it is important to contemplate the influence of parameter uncertainty.

With regard to the pile group behaviour, most of the available literature and the past research are pertinent to conventional deterministic studies. Very few literatures are relating to the uncertainty analyses or the parameter uncertainty in specific are seldom available. Lacasse and Goulois [20] reviewed the necessity of considering the uncertainty of soil properties with the emphasis on shallow and pile foundations. Halder and Babu [21] studied the effect of spatially varying soil on the lateral response of a pile in cohesive soil using the finite-difference method in FLAC. Naghibi et al. [22] investigated the finite-element-based differential settlement behaviour of a two-pile foundation via Monte Carlo simulation with the probabilistic consideration. Hamrouni et al. [23] proposed a finite-difference based axisymmetric model of an earthen platform improved by vertical piles using FLAC considering the soil properties as random variables following the normal distribution.

Leung and Lo [24] performed the reliability analyses of pile foundations in the spatially varying soil and observed the significant interaction between superstructure stiffness and soil uncertainty. Halder and Chakraborty [25] studied the influence of inherent spatial variation of soil parameters in the behaviour of strip footing lying on a geocell-reinforced slope. The probabilistic factor of safety is determined using the combination of random field methodology with FLAC.

Hamrouni et al. [26] determined the bearing capacity of a shallow foundation under pseudo-static conditions in the reliability-based finite-difference framework using FLAC. The authors have considered the horizontal seismic coefficient, soil's cohesion and internal angle of friction as the

random variables in the study. Minnucci et al. [27] carried out the probabilistic investigation on the pile groups considering the soil parameters—soil density as in normal distribution, shear wave velocity, and Young’s modulus as in lognormal distribution as random variables in the seismic analyses of pile groups. Song et al. [28] presented the methodology to determine the design parameters of energy piles by considering the parameter uncertainty of soil in the stochastic domain. Kotra and Chatterjee [29] investigated the effect of spatial correlation in the cone penetration resistance data in determining the analytical pile group capacity. Kotra and Chatterjee [30] studied the effect of uncertain friction angle of soil on the lateral response of pile group using finite-difference methodology in FLAC3D [31] and reviewed the stochastic responses of lateral deflection profiles accordingly.

Based on the above-mentioned research studies, it is evident that the soil parameters such as cohesion, friction angle, horizontal seismic coefficient, shear wave velocity, Young’s modulus, and superstructure stiffness were taken as random variables to address the uncertainty studies relating to the pile group. And the research relating to the pile groups subjected to the combined axial and lateral loading in the domain of parameter uncertainty are scarce. Hence the present study is devised in a way to address the uncertainty associated with the soil Young’s modulus for a pile group problem embedded in sandy medium. In the present study, the elastic Young’s modulus following the lognormal probability distribution is contemplated. In this 2 × 2 pile group problem, the resulting soil reaction profiles i.e., *p*-*y* curves for the lateral load applications are examined along the various depths of front pile and rear pile are studied. The incurring variability in the behaviour of the soil-pile foundation system is exemplified using the stochastic representations.

Framework and Methodology of Analyses

Finite-Difference Modelling

The analysis methodology involved by means of the three-dimensional finite-difference method i.e., FLAC3D. The finite-difference approach utilizes the first-order based space and time derivatives. They are approximated by the finite differences with the assumption of linear variations of pertaining variables over its finite spaces and time intervals. The FLAC3D considers node as the prime object for the computation of force and the mass. The equations of motion are transformed into the discrete space of Newton’s law at all the nodes. The generated system of equations is mathematically solved through the explicit method of finite-difference approach in the time-domain. The following equation of Newton’s law and its finite-difference form through the recurrence relation at the elemental nodes can be written as

$$F_i^l = M^l \left(\frac{\partial v_i}{\partial t} \right)^l \tag{1}$$

$$\frac{\partial v_i^l}{\partial t} = \frac{F_i^l(t) + f_i^l(t)}{M^l} \tag{2}$$

$$v_i^l \left(t + \frac{\Delta t}{2} \right) = v_i^l \left(t - \frac{\Delta t}{2} \right) + \frac{\Delta t}{M^l} (F_i^l + f_i^l) \quad \text{for, } l = 1 \dots n_n \tag{3}$$

where *f_i^l* is the damping force and it is generally expressed as the out-of-balance force *F_i^l*, *v_i* is the grid point velocity and *M* is mass of the node.

In the same manner, the updated node displacements (with *u_i^l* = 0) and node location can be obtained using the central finite-difference approximation shown as follows:

$$u_i^l(t + \Delta t) = u_i^l(t) + \Delta t v_i^l \left(t + \frac{\Delta t}{2} \right) \tag{4}$$

$$x_i^l(t + \Delta t) = x_i^l(t) + \Delta t v_i^l \left(t + \frac{\Delta t}{2} \right) \tag{5}$$

With the traction vector [*t*] and a unit normal [*n*] on any face, *σ_{ij}* as the stress tensor, *b_i* as the body force and *ρ* as the mass density, the stress at a particular point can be characterized by using the Cauchy’s formulation as

$$t_i = \sigma_{ij} n_j \tag{6}$$

$$\frac{\partial \sigma_{ij}}{\partial x_i} + \rho b_i = \rho \frac{\partial v_i}{\partial t} \tag{7}$$

The strain increment, *Δe_{ij}* based on the nodal velocities can be obtained as

$$\Delta e_{ij} = \frac{1}{2} (v_{i,j} + v_{j,i}) \Delta t \tag{8}$$

With *σ̂_{ij}* as the stress rate tensor, the constitutive formulations were then utilized in the corresponding incremental form *H_{ij}^{*}* and solved using mathematical iterations to obtain the new stresses and the final solution

$$\sigma_{ij}^{\wedge} = H_{ij}^* (\sigma_{ij}, \Delta e_{ij}, k) \tag{9}$$

where *k* is the loading history parameter.

Numerical Simulation of a 2 × 2 Pile Group

In the current study, the surrounding soil medium is modelled using the eight-node brick zones, the piles and the pile cap were modelled using the ‘structure-pile’ beam elements and ‘shell’ element, respectively. The size of each soil brick

zone is assessed by performing a few initial analyses such that the change in the geostatic stresses is insignificant after its increase. The side lateral boundaries of the model are fixed in their respective lateral directions and bottom boundary is restrained for the displacements. In the first stage, the geostatic stresses for the surrounding soil medium are generated by the virtue of its properties under the gravitational loading and then it is set to an equilibrium state. In the next stage, the pile group installation is modelled by using structure-pile element and the corresponding normal and shear stiffnesses are attached at the soil-pile interface nodes. The model is set into equilibrium after installing the pile group with the corresponding properties. After performing these initial steps, the pile group is then combinedly loaded in vertical and lateral directions onto the pile cap simultaneously.

Modelling of Soil-Pile Interface

In FLAC3D, the constitutive relation for the soil-pile interface is considered as a linear Coulomb shear-strength model and is represented as [31],

$$F_s^{\max} = c_i A + \tan_i (F_n - p_i A) \quad (10)$$

In the above equation, F_s^{\max} and F_n are the shear force and the normal force acting at the soil-pile interface, respectively; c_i and ϕ_i are the alongside cohesion and friction angle, respectively, p_i is the generated pore pressure and A is the area pertaining to the node at the interface. In the current study, the soil is cohesionless and so, c_i is zero and only the friction angle defines the shear strength. For the interface node, the normal force is determined by Eq. (2) and the shear force is determined by Eq. (3)

$$F_n^{t+\Delta t} = k_n u_n A + \sigma_n A \quad (11)$$

$$F_{si}^{t+\Delta t} = F_{si}^t + k_s \Delta u_{si}^{t+0.5\Delta t} A + \sigma_{si} A \quad (12)$$

In above Eqs. (2) and (3), F_{si} , k_n and k_s are the shear force, normal stiffness and shearing stiffness, respectively; Δu_{si} is the displacement vector with respect to shear, u_n is normal displacement of the node at the interface, σ_n and σ_{si} are the vectors of normal stress and shear stress initialized by the interface stresses at the nodes. In modelling the soil-pile interface, the coupling springs are attached in the vertical and lateral directions at each and every pile node. The magnitude of interfacial friction angle is taken as 2/3 times the surrounding soil's friction ϕ . Chatterjee et al. [32, 33] utilized the following formulations for determining k_n and k_s as follows [34]

$$k_n = \frac{4Gr_0}{1-\nu} \quad (13)$$

$$k_s = \frac{32(1-\nu)Gr_0}{7-8(1-\nu)} \quad (14)$$

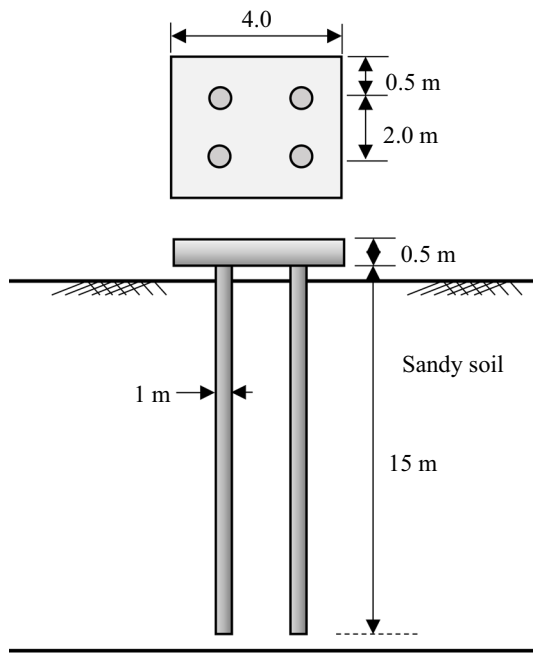
where G , ν and r_0 are the shear modulus, Poisson's ratio and pile's radius, respectively.

Validation of the Numerical Model

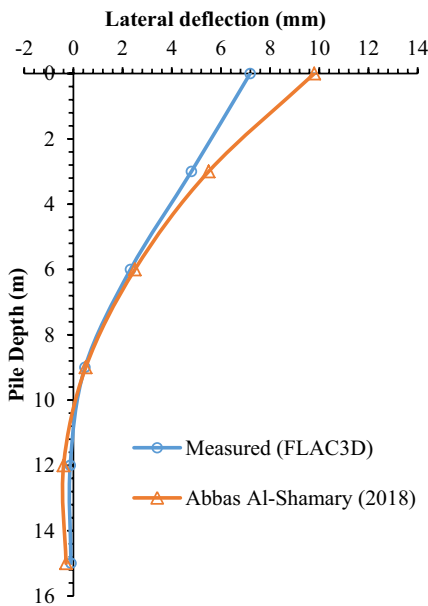
A 2×2 pile group model is modelled in FLAC3D based on Abbas Al-Shamary et al. [35]. The cohesionless soil medium following the Mohr–Coulomb's model is used in the validation study. The soil properties such as the friction angle, ϕ is taken as 30° , unit weight as 20.0 kN/m^3 , elastic modulus as 13.0 GPa and the circular pile section with length as 15 m , diameter of 1.0 m and the pile cap of 0.5 m height is considered in this validation study. The thickness of the pile cap is 0.5 m . The distance between the pile cap and the ground surface is kept to 0.5 m . The central spacing between the piles is taken as two times the diameter of the pile i.e., 2 m . The schematic view of the pile group is shown in Fig. 1a. The initial steps of pile group installation are executed as per the methodology explained in the earlier sections. For validation purposes, the same lateral load of 450 kN is applied uniformly on the pile group and the response is compared as shown in Fig. 1b. It is observed that the numerical model adopted in the present validation study exhibits a favourable agreement with regard to the deflection profile.

Present Study

In the current study, the 2×2 pile group is embedded in a homogeneous sandy soil of medium density. The numerical model comprising the pile group installation is executed in FLAC3D as explained in the preceding sections. The cohesionless soil medium is modelled with the elastic Mohr–Coulomb plastic constitutive formulation in this study. The soil properties such as, the elastic modulus E , bulk modulus K , shear modulus G , and the friction angle ϕ , given in Table 1 are utilized in the study. In order to converge the numerical model, the cohesion intercept c , of the soil is kept to the least value of 1 kPa . The properties and details of the pile cap and pile elements include, diameter, length, Shear modulus G , bulk modulus K , and density ρ are shown in Table 2. The piles are modelled utilizing structure-pile elements and the pile cap utilizing the shell elements available in FLAC3D as explained earlier. The size of each eight-node brick element is adjusted to a fairly small, such that the geostatic stresses in the elements are approximately



(a) schematic view of a 2×2 pile group



(b) lateral deflection profile

Fig. 1 Validation study **a** schematic view of a 2×2 pile group **b** lateral deflection profile (after Abbas Al-Shamary [35])

same even after decreasing this size. Besides the model convergence associated with the various stages of the numerical model, the mesh size is adjusted in a way to influence the results minimally. Based on the initial trials, the suitable size of brick element is found to be 0.25 and the same size is assigned to all the elements in lateral x , y and the vertical

Table 1 Soil properties used in the study (modified after Hazzar et al. [9] and Bowles [39])

S. No	Soil property	Value
1	Density, ρ_s (kg/m ³)	2000
2	Angle of internal friction, ϕ (°)	60
3	Shear modulus, G_s (kN/m ²)	19.2×10^3
4	Elastic modulus, E_s (kN/m ²)	49.92×10^3
5	Poisson's ratio, ν_s	0.3
6	Relative density, D_r (%)	45
7	COV of E_s (%)	10, 20, 30

Table 2 Dimensions of pile group model and its properties

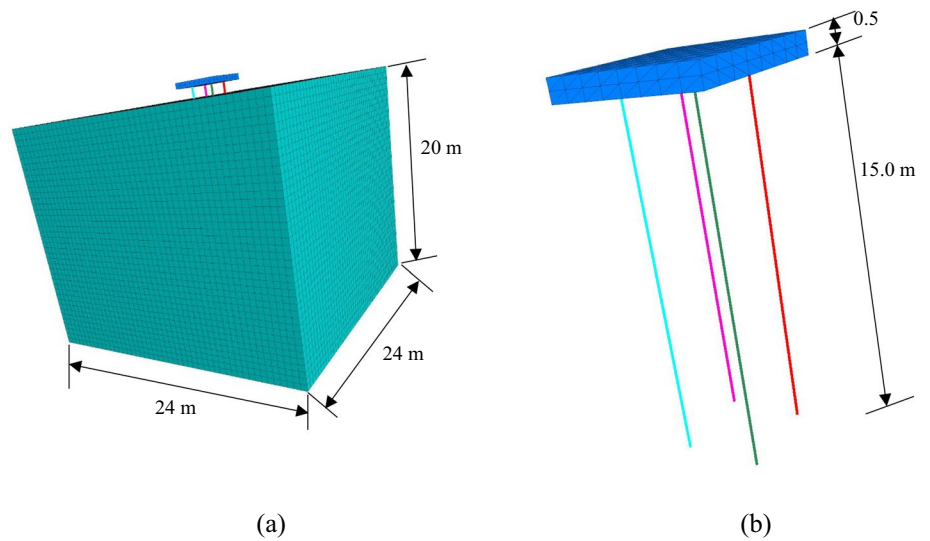
S. No	Parameter	Value
1	Pile length, L	15.0 m
2	Cross section, D	1.0 m
3	No. of piles	4
4	Pile cap	4.0 m × 4.0 m
5	Thickness of cap	1.0 m
6	Density, ρ_p	2500 kg/m ³
7	Elastic modulus	25 GPa
8	Poisson's ratio, ν_p	0.20
9	Spacing between piles	2D (centre to centre)

z directions of the numerical model. Considering D as the diameter and L as the length of the pile, the total height of the homogeneous soil is set to $L + 5D$ and the side lateral boundaries are extended to $10D$ in both the x and y directions of the numerical model as shown in Fig. 2. The lateral boundaries of the model are fixed in their respective lateral directions and bottom boundary is restrained for the displacements. With regard to the pile cap, it is considered as a flexible element which is modelled by creating the brick elements first, and then the elements are associated with that of shell element. The flexible pile cap thus allows the differential movement between the piles in the group. The varied lateral deflection and bending moment profiles in both the front and rear piles are discussed in the succeeding sections.

Application of Combined Axial and Lateral Load Onto the 2×2 Pile Group

After the initial steps of 2×2 pile group installation and attaining its equilibrium as said in the earlier sections, the vertical load over the pile cap and the lateral load at the side of the pile cap is applied as the uniformly distributed load onto the considered pile group model. The ultimate load-carrying capacity based on IS 2911 [36] of the pile group V_{ult} was determined to be 13,000 kN. The axial loading (V) i.e., $V = V_{all}$, which is the allowable load

Fig. 2 A 2×2 pile group model used in the study **a** soil block **b** pile group with cap



calculated by dividing the V_{ult} with the factor of safety of 3.0 is applied for the current numerical model. The lateral load (Q) in four distinct combinations, i.e. $Q = 0.25 V$, $0.5 V$, $0.75 V$ and $1.0 V$ are then applied at the side of the pile cap. Regarding the application of load, the axial load is applied first, and then the lateral load is applied; both the loads are applied as the uniformly distributed load on the pile cap. The resulting p - y curves generated through the lateral soil reaction at the different depths of pile were then recorded using FISH programming in FLAC3D.

Inclusion of Parameter Uncertainty—Elastic Modulus of Soil

In the present study, the Young’s or the elastic modulus E , of the soil is considered as the uncertain parameter to examine the bending moments, deflection profiles and the p - y behaviour of the pile group. The present stochastic parameter E is associated with the lognormal distribution in the current work [17, 18]. In the literature, the elastic modulus is taken as a random variable with the COV of 30% by Paice et al. [37] and 20–70% is taken by Phoon and Kulhawy [17, 18, 38]. The study present is performed with the COVs of 10%, 20% and 30% which lies within the range as mentioned in Paice et al. [37] and Phoon and Kulhawy [17, 18]. The Monte Carlo method works on the principle of repetitive random sampling that considers the uncertainty pertaining to the input parameters with their specific probability distribution in the model [16]. The Monte Carlo method then determines the probability distribution of the results obtained for all the runs or realizations of COVs. The cumulative mean of soil’s elastic modulus was calculated for 2000 random samples generated for the Monte Carlo method initially. The cumulative

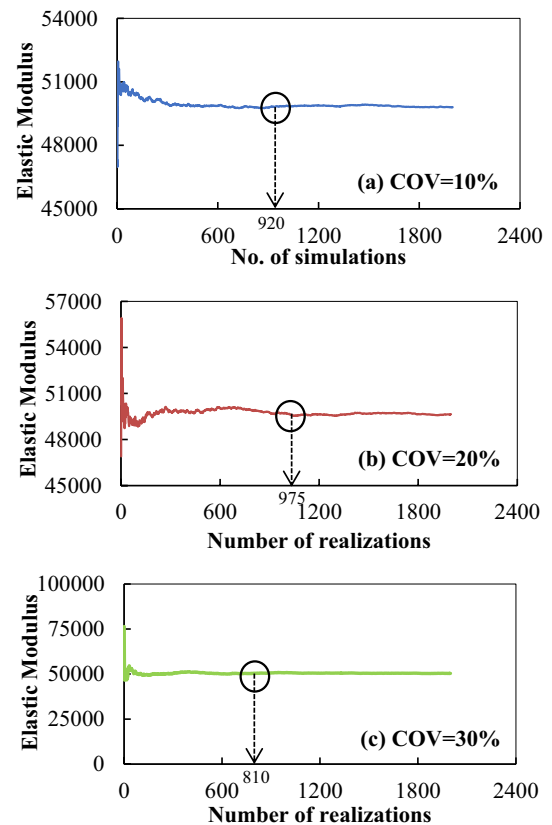
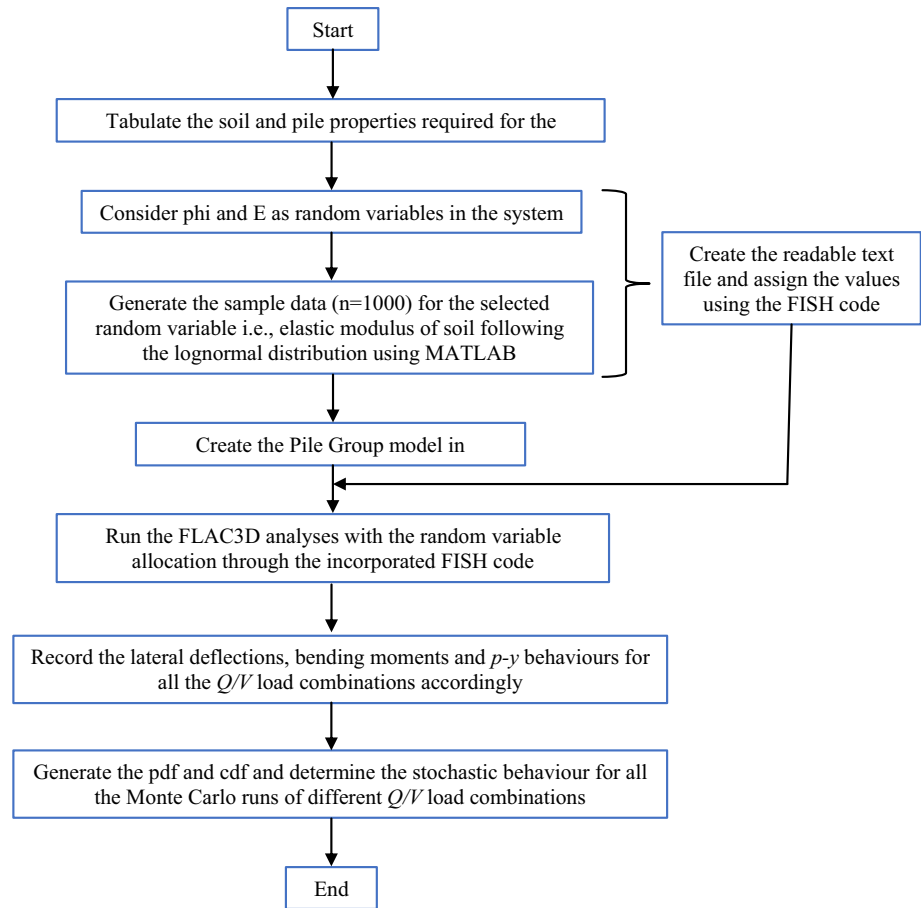


Fig. 3 Cumulative mean of soil’s Elastic modulus for the generated random samples

elastic modulus becomes stable and approximately equal to the considered mean value after 920 samples for COV of 10%, 975 samples for COV of 20% and 810 samples for COV of 30% as depicted in the convergence study (Fig. 3). Thus, a thousand lognormal random samples of E were generated in MATLAB for each COV of 10%, 20%

Fig. 4 Flowchart representing the methodology followed in the study



and 30% and each value is assigned for every simulation of the load combination using FISH (inbuilt in FLAC3D). The resulting probability density function (pdf) and cumulative density function (cdf) were then illustrated for bending moments and lateral deflection profiles for each load combination. The influence of COV of E on the p - y responses at different depths of pile is also presented in the later sections. The methodology followed in the determining the stochastic behaviour of the pile group responses is depicted with the flowchart in Fig. 4.

Results and Discussion

The influence of the combined axial load and the lateral load on the pile group is analysed in the current study. The findings of this study are shown as deterministic and statistical profiles for the bending moments, lateral deflections and the incurring p - y curves at different depths of the piles. Figures 5 and 6 display the deterministic variation of the bending moments and lateral deflection profiles for the various Q/V load combinations, respectively.

Deterministic Bending Moment and Lateral Deflection Profiles

From Fig. 5, it can be observed that the magnitudes of bending moments are higher in the case of front pile when compared to the rear pile. For the load combination of $Q/V=0.25$, the maximum bending moment for the front and rear piles are found as 28.2 kNm and 18.4 kNm, respectively. For the load combination of $Q/V=0.5$, the maximum bending moment for the front and rear piles are found as 40.1 kNm and 29.3 kNm. For the load combination of $Q/V=0.75$, the maximum bending moment for the front and rear piles can be found as 53.2 kNm and 42.8 kNm, respectively. For the load combination of $Q/V=1.0$, the maximum bending moment for the front and rear pile can be found as 65.1 kNm and 59.4 kNm, respectively. It can be observed that, with the increase in the lateral load the maximum bending moment also increases for all the Q/V load combinations accordingly.

From Fig. 6, it can be seen that, the lateral deflection is maximum at the top of the pile for all the load combinations in both the front and rear piles. The maximum lateral deflection is more in the front pile when compared to the rear pile

Fig. 5 Bending moment profiles of piles **a** front pile **b** rear pile

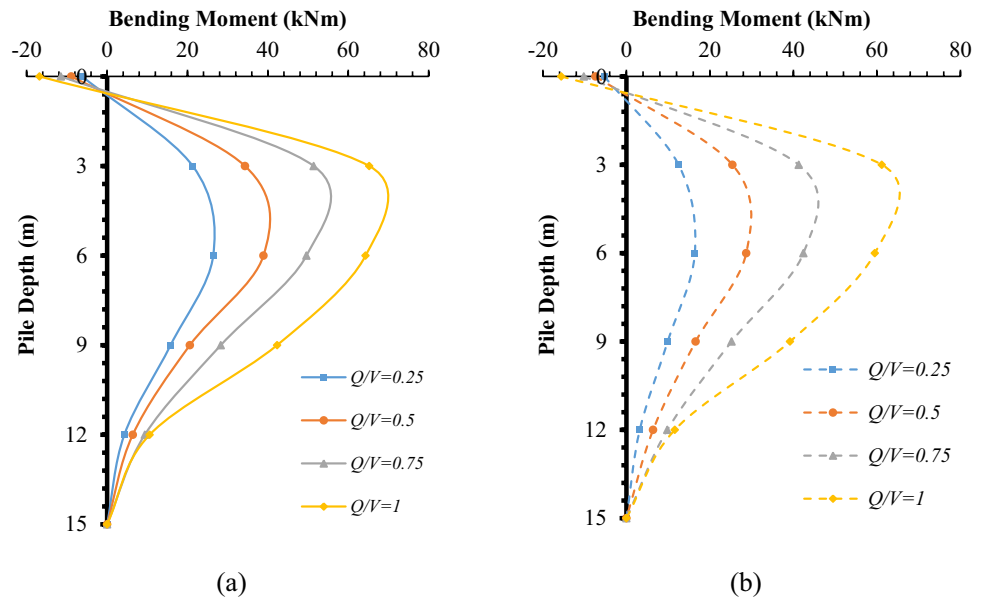
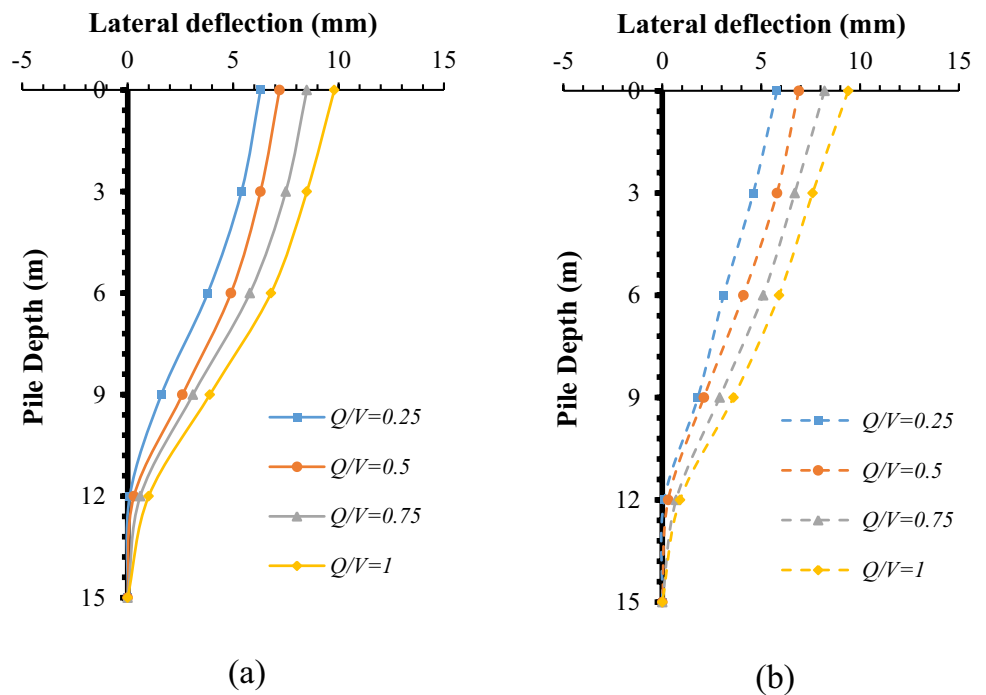


Fig. 6 Lateral deflection profiles of piles **a** front pile **b** rear pile



in all the Q/V load combinations. This occurrence is attributable to the shadow effect in the pile group.

Stochastic Responses

In the present study, as said earlier, the ten-thousand runs of each load combination are performed to study the stochastic behaviour i.e., the probability density function (pdf) and the cumulative density function (cdf) of the bending moment and lateral deflection profiles for all the Q/V load

combinations. The pdf and cdf responses are determined for every COV of elastic modulus of soil (10%, 20% and 30%). The Monte Carlo method produces the bending moment profiles for the COV of 10% as the stochastic representations as given in Fig. 7 for the front pile and Fig. 8 for the rear pile; the lateral deflection profiles are given in Fig. 9 for the front pile and Fig. 10 for the rear pile.

The Monte Carlo simulations considering the uncertainty in elastic modulus, produce the lateral deflection profiles for

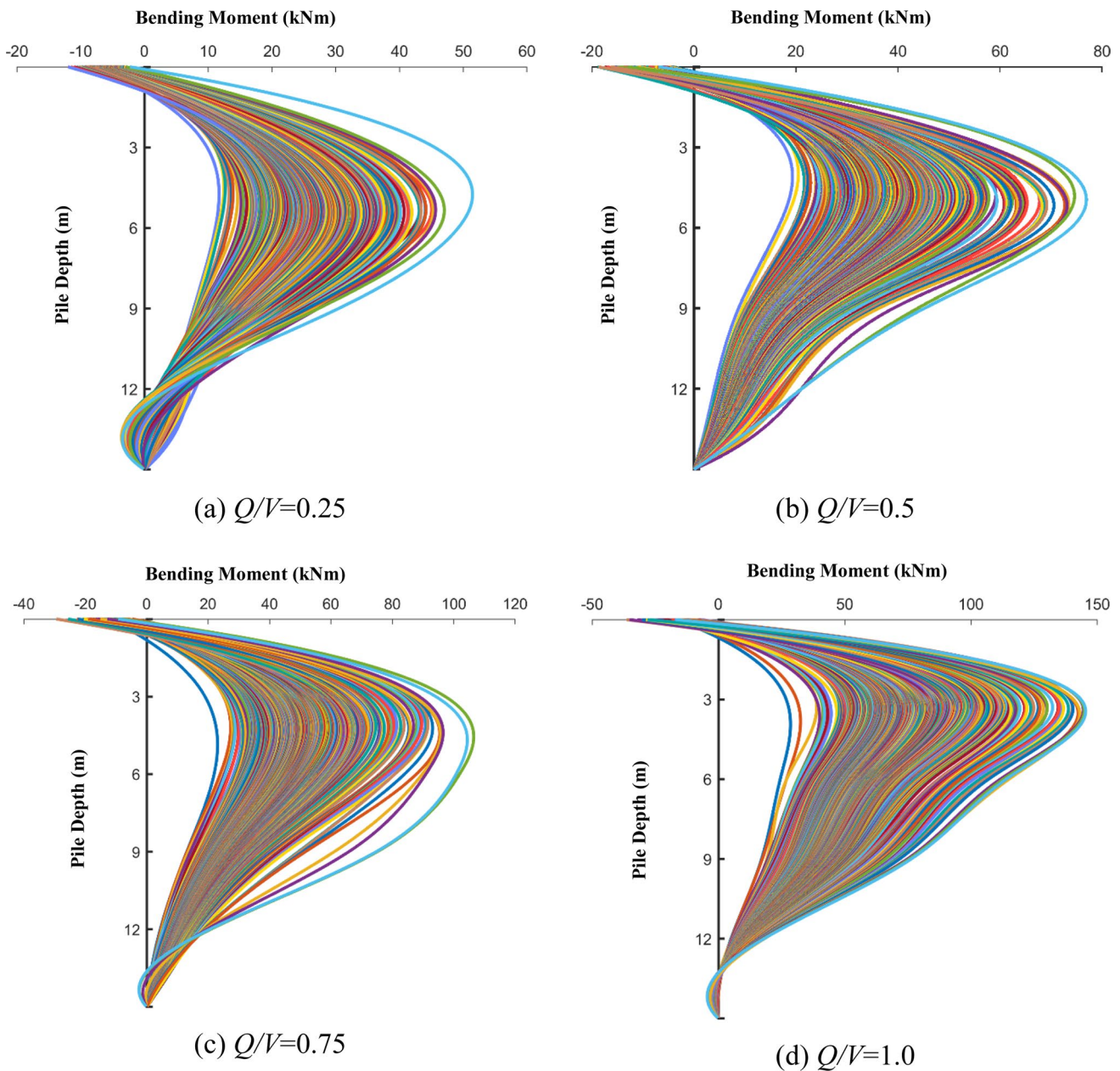


Fig. 7 Bending moment profiles for all the realizations—front pile

the COV of 10% are shown in Fig. 9 for the front pile and Fig. 10 for the rear pile.

The stochastic responses i.e., the pdf and cdf illustrations for the maximum bending moments and maximum lateral deflections of the front and rear piles for all the Q/V combinations are presented in Figs. 11, 12, 13, 14, 15, 16, 17, 18.

The relative cdfs generated for the different Q/V combinations illustrate the importance of pile group bending moments and lateral deflections with the consideration of parameter uncertainty in the elastic modulus of soil. For the front pile, the 50% probability of occurrence of maximum

bending moment decreases for about 9.1% when the COV increases from 10% to 30%, whereas for the Q/V of 0.5, the decrease is 8.69%, for the Q/V of 0.75, the decrease is 10.7% and for $Q/V=1.0$, the decrease is 10.9%. In the case of rear pile, for the Q/V combination of 0.25, the 50% probability of occurrence of maximum bending moment decreases for about 14.3% when the COV increases from 10% to 30%, whereas for the Q/V of 0.5, the decrease is 8.8%, for the Q/V of 0.75, the decrease is 15.5% and subsequently for $Q/V=1.0$, the decrease is 8.33%. Apart from the probability of occurrence of 50%, the percentage increase

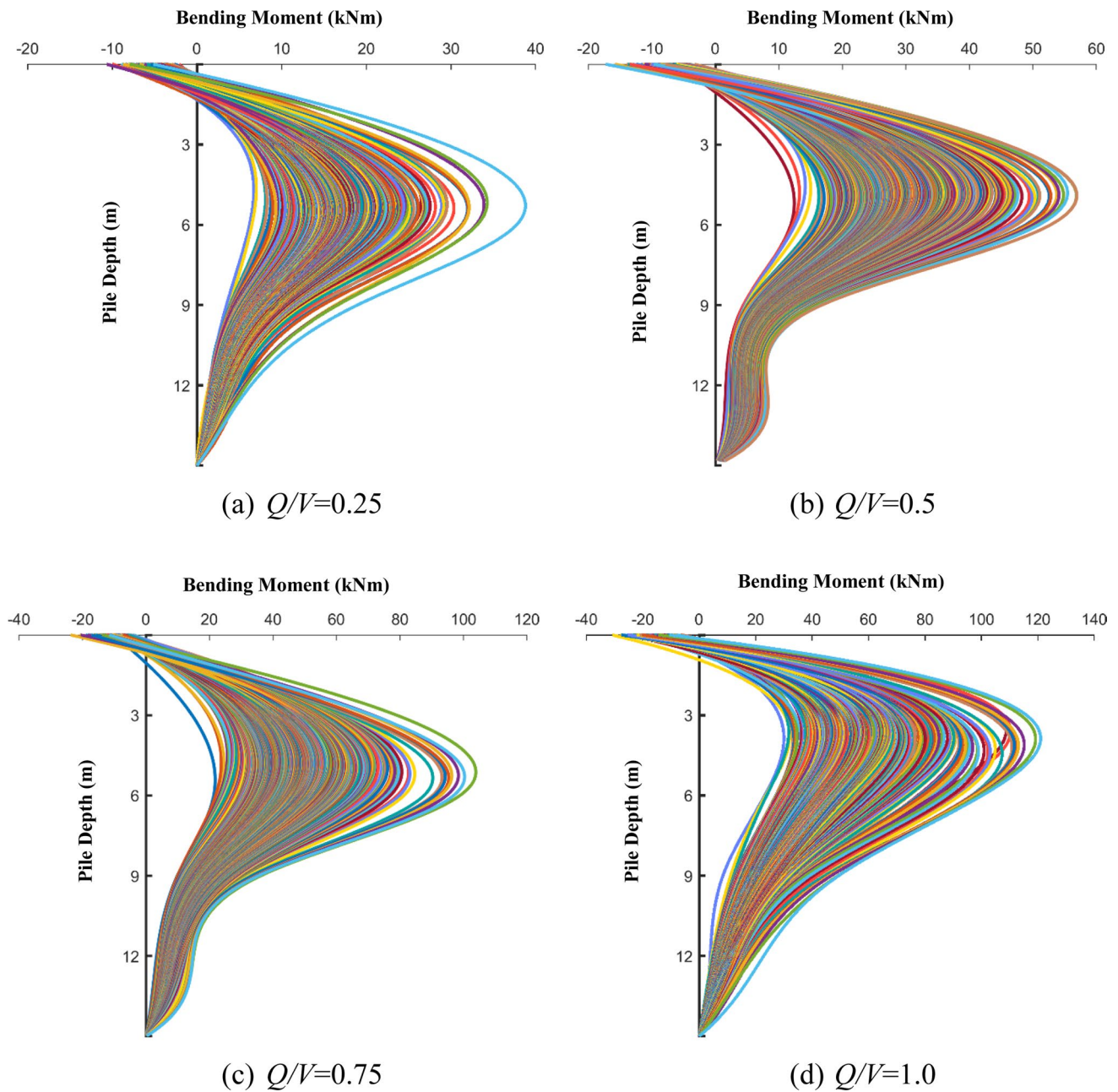


Fig. 8 Bending moment profiles for all the realizations—rear pile

in the magnitude of the difference in the maximum bending moments can be observed from the cdf illustrations presented in Figs. 12, 14.

The influence of COV of elastic modulus on the stochastic response of all the maximum bending moments for all the Q/V combinations is listed in Table 3 for the COV of 10%, Table 4 for the COV of 20% and Table 5 for the COV of 30% along with the standard deviation (SD). It is observed that, the maximum COV of the responses is in the increasing trend proportionately with the input COV. Among all

the responses, the maximum COV of the responses is found to be as 34% for the Q/V of 0.5 with the input COV of 30%.

For the front pile, the 50% probability of occurrence of maximum lateral deflection decreases for about 10% when the COV increases from 10% to 30%, whereas for the Q/V of 0.5, the decrease is 4.2%, for the Q/V of 0.75, the decrease is 6.3% and for $Q/V=1.0$, the decrease of 3.2% are observed. In the case of rear pile, for the Q/V combination of 0.25, the 50% probability of occurrence of maximum lateral deflection decreases for about 11.3% when the COV increases from 10% to 30%, whereas for the Q/V of

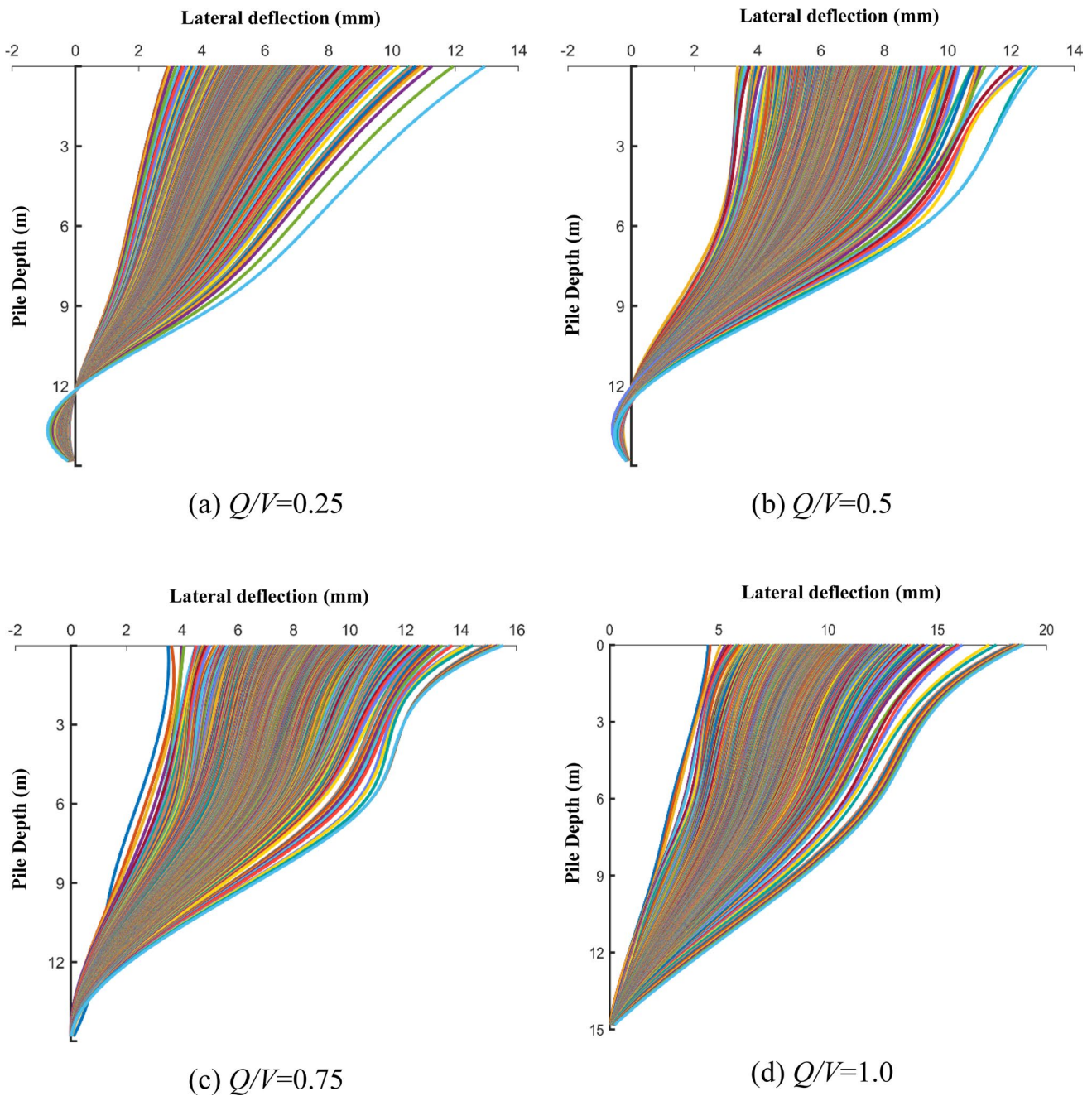


Fig. 9 Lateral deflection profiles for all the realizations—front pile

0.5, the decrease is 6.8%, for the Q/V of 0.75, the decrease is 7.9% and further for $Q/V = 1.0$, the decrease of 4.1% are observed. For both the front and rear piles, the variation in the maximum lateral deflection can be observed when the probability of occurrence is increased to the higher magnitudes and it can be understood by the concerned cdf illustrations as given in Figs. 16, 18.

The influence of COV of elastic modulus on the stochastic response of all the maximum lateral deflections for all the Q/V combinations is listed in Table 6 for the COV

of 10%, Table 7 for the COV of 20% and Table 8 for the COV of 30%. It is observed that, for the maximum lateral deflections, the COV of the responses is in the increasing trend proportionately with the input COV. Among all the responses, the maximum COV of the responses is found to be as 31% for the Q/V of 1.0 for the front pile with the input COV of 30%.

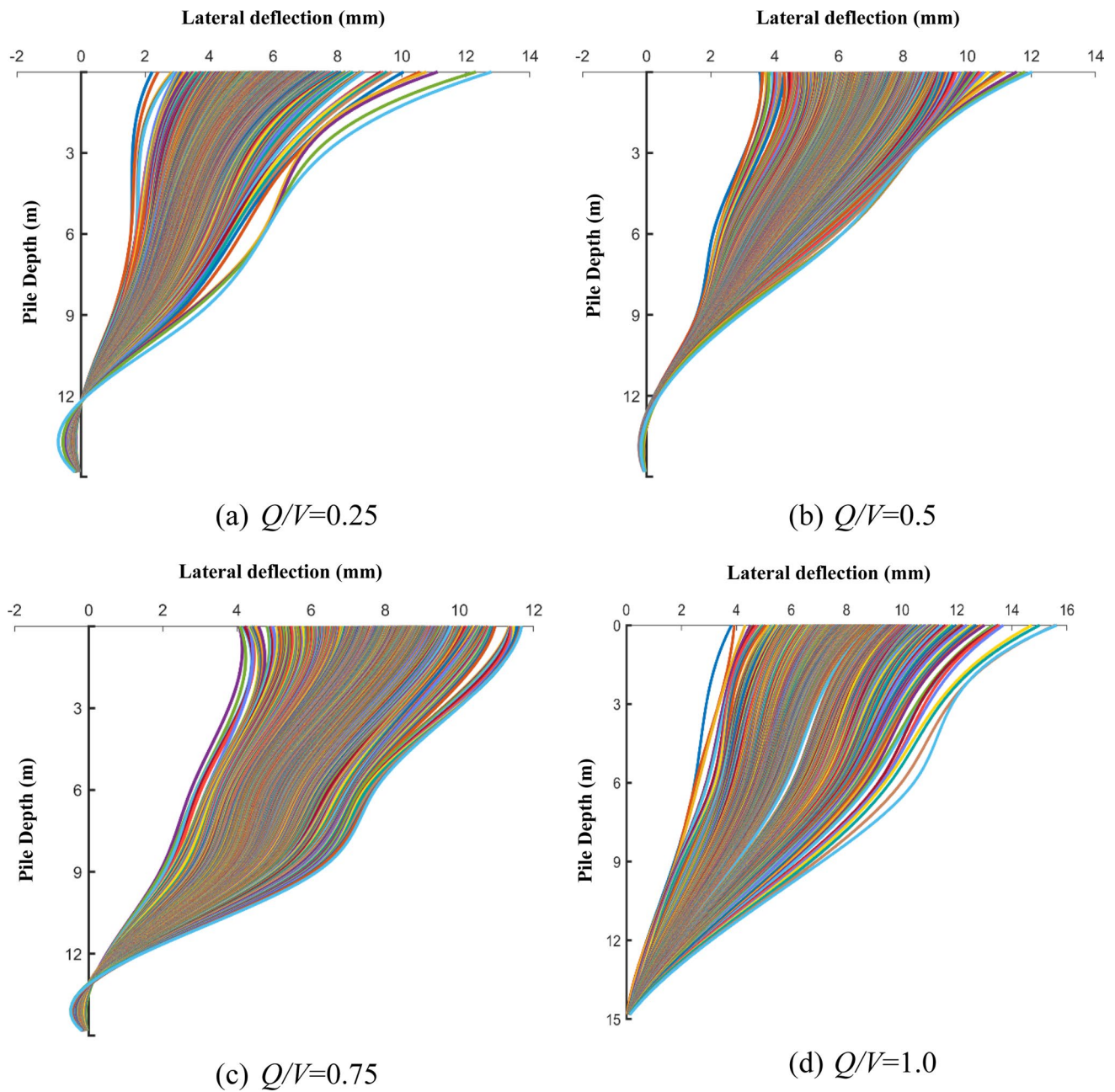


Fig. 10 Lateral deflection profiles for all the realizations—rear pile

p-*y* Curves

As a result of applying the lateral load to the pile group, the resistance generates in the soil medium surrounding the pile and the magnitude is recorded through the FISH (inbuilt in FLAC3D) using the forces generated at the concerned pile depth. The deterministic variation of the soil reaction along the depths of the pile is shown in Fig. 19

for the front pile and Fig. 20 for the rear pile. Each coordinate on the curve represents the response of each Q/V load combination and all these responses are recorded at 3 m, 6 m, 9 m and 12 m depths of the front and rear piles. At a particular depth of the pile, it is evident that the soil reaction increases with the rising Q/V ratio in both the front and rear piles. It can also be observed that, for the same load combination, the magnitudes of the soil reaction

Fig. 11 Probability density function of bending moments—front pile

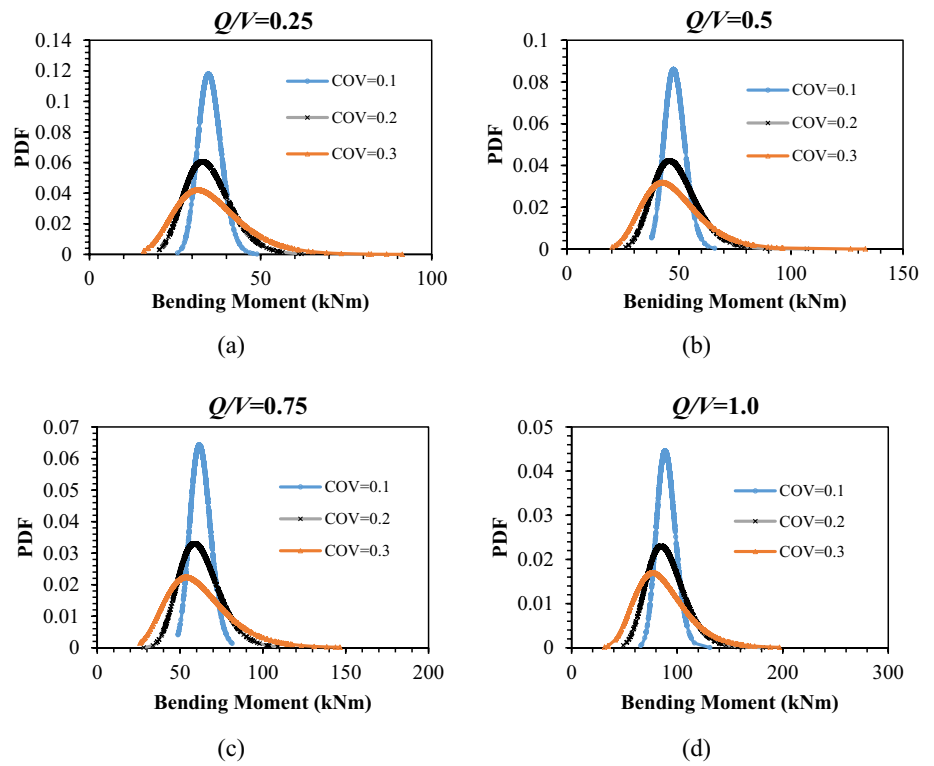


Fig. 12 Cumulative density function of bending moments—front pile

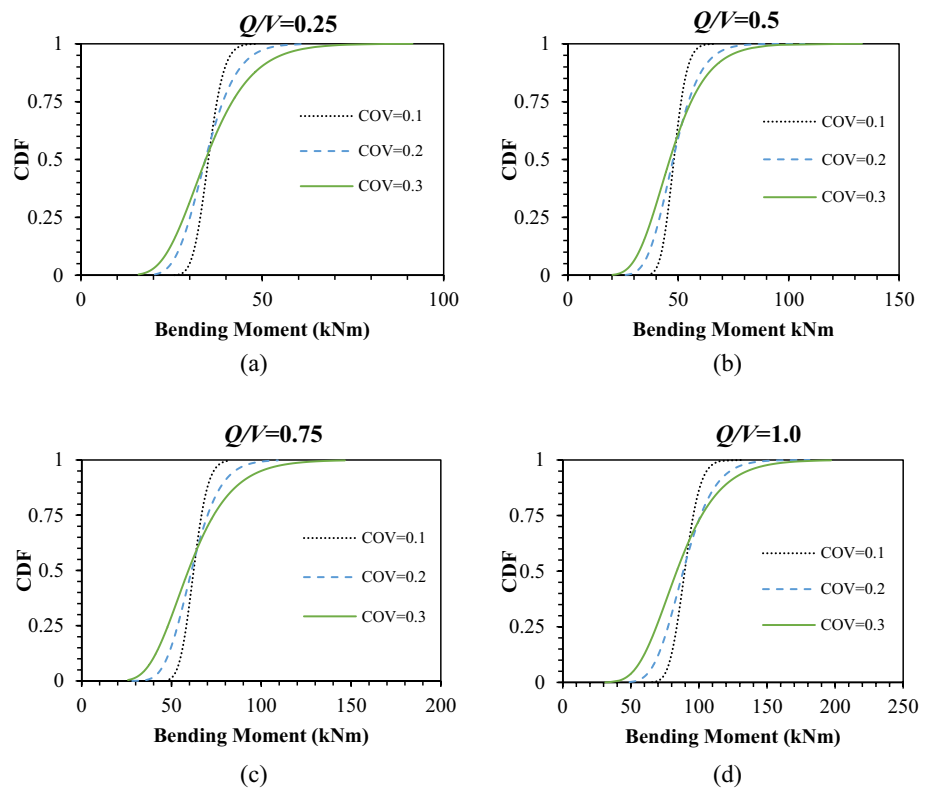


Fig. 13 Probability density function of bending moments—rear pile

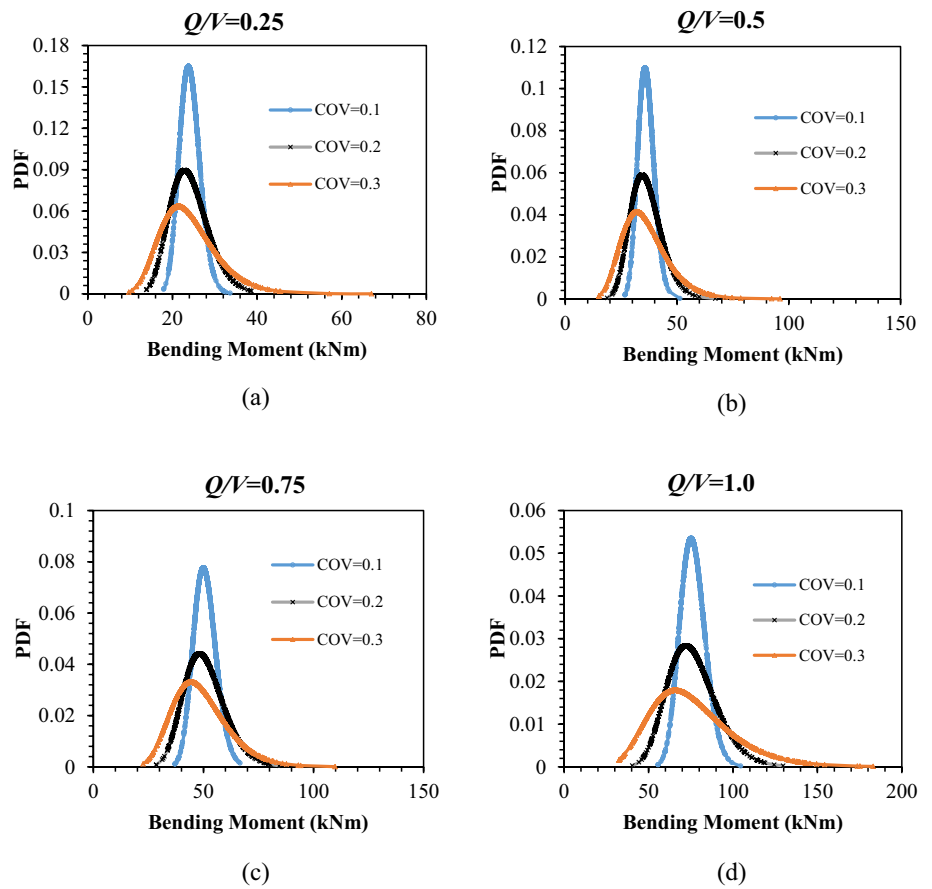


Fig. 14 Cumulative density functions of bending moments—rear pile

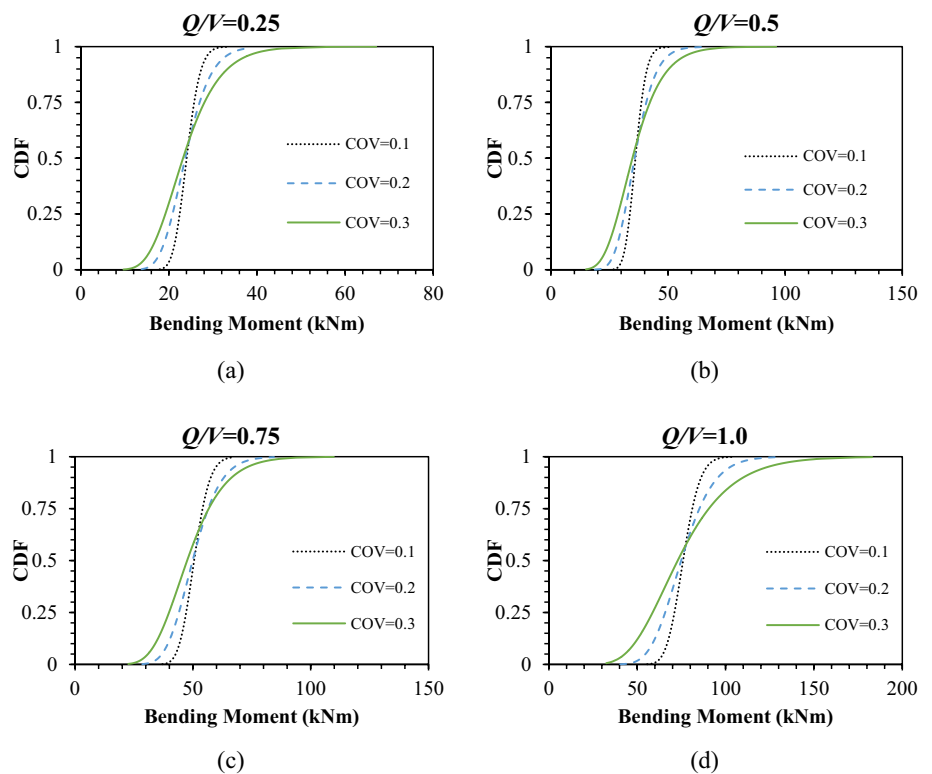


Fig. 15 Probability density function of lateral deflections—front pile

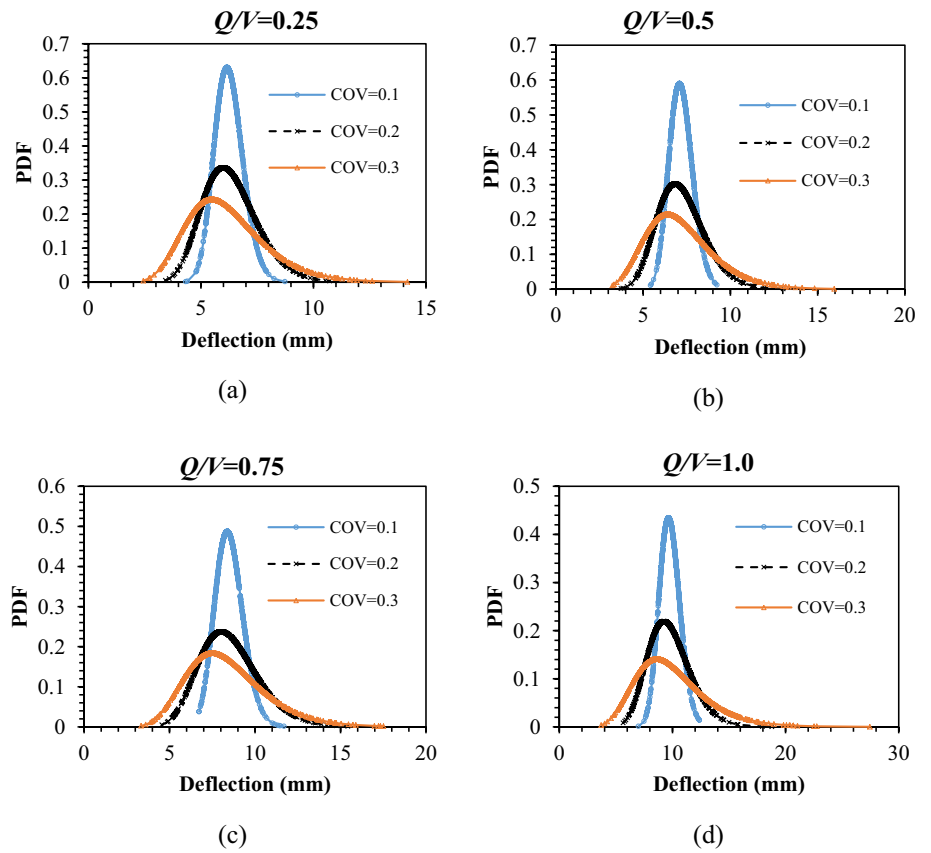


Fig. 16 Cumulative density functions of lateral deflections—front pile

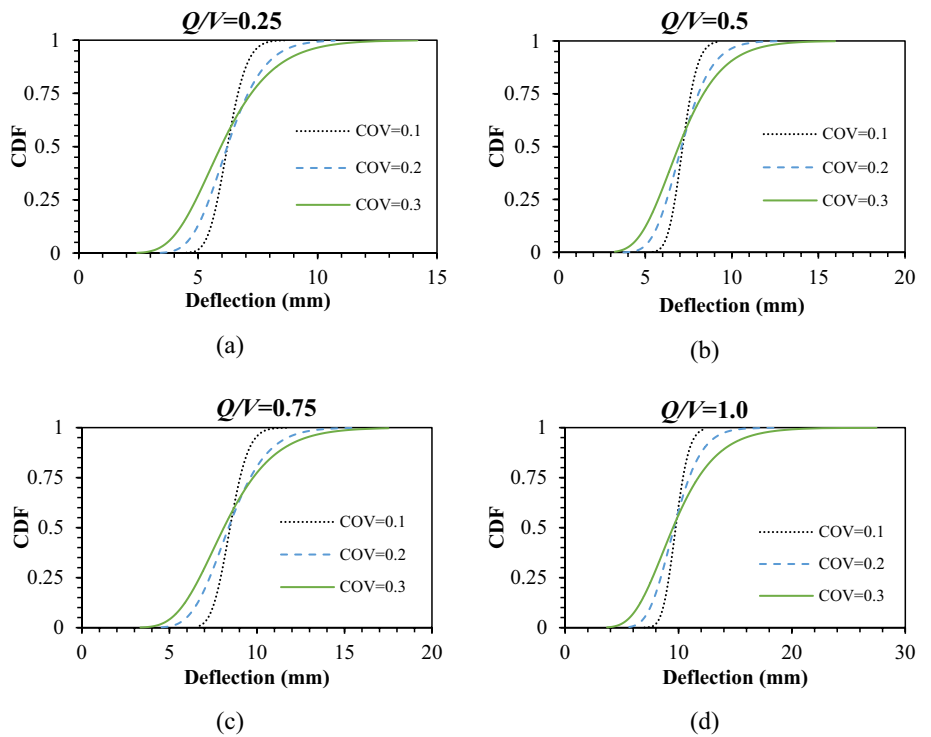


Fig. 17 Probability density function of lateral deflections—rear pile

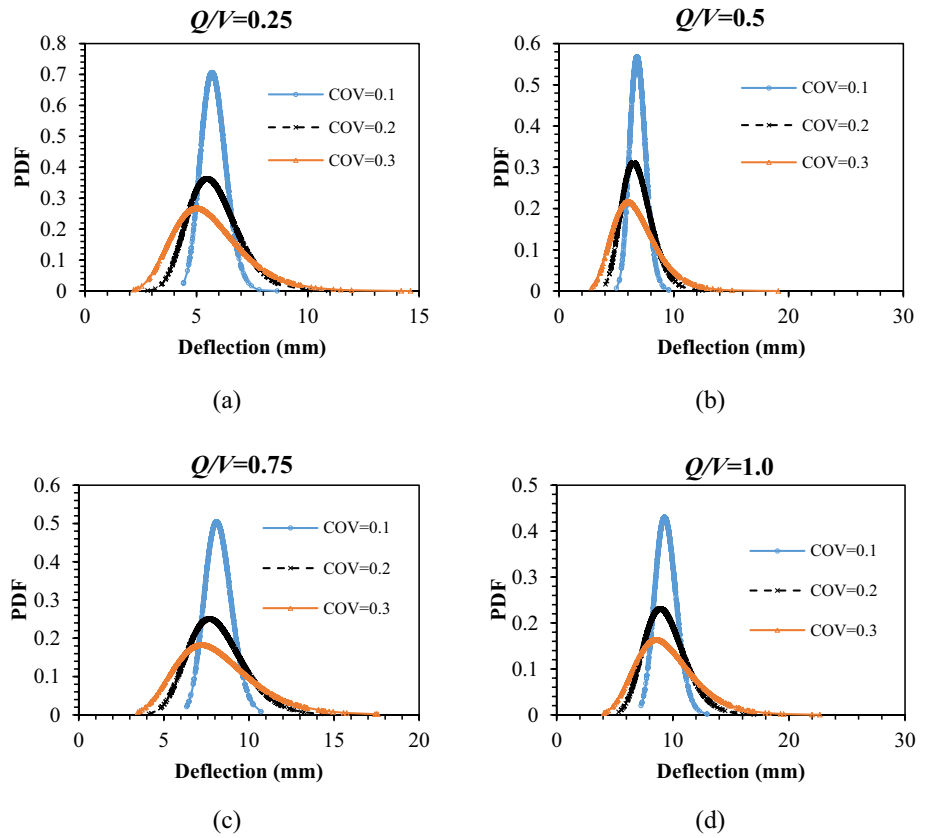


Fig. 18 Cumulative density functions of lateral deflections—rear pile

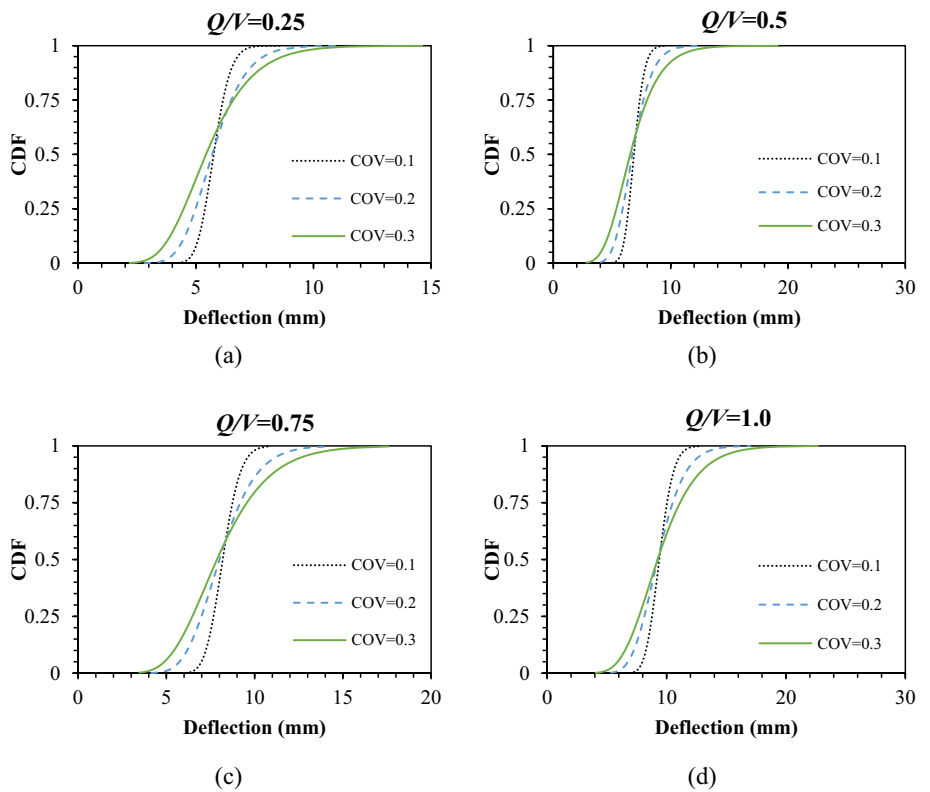


Table 3 Stochastic responses of the maximum bending moments of pile group with the input COV of 10%

COV = 10% Q/V	Front pile			Rear pile		
	Mean	SD	COV	Mean	SD	COV
0.25	35.4	3.89	0.11	26.3	4.20	0.16
0.5	50.2	6.52	0.13	37.8	6.80	0.18
0.75	63.1	11.35	0.18	53.7	9.12	0.17
1	88.7	21.28	0.24	71.6	11.45	0.16

Table 4 Stochastic responses of the maximum bending moments of pile group with the input COV of 20%

COV = 20% Q/V	Front pile			Rear pile		
	Mean	SD	COV	Mean	SD	COV
0.25	33.8	5.40	0.16	23.7	4.50	0.19
0.5	48.7	13.14	0.27	34.1	8.86	0.26
0.75	58.2	13.38	0.23	45.6	10.94	0.24
1	77.6	14.74	0.19	67.3	14.13	0.21

Table 5 Stochastic responses of the maximum bending moments of pile group with the input COV of 30%

COV = 30% Q/V	Front pile			Rear pile		
	Mean	SD	COV	Mean	SD	COV
0.25	31.6	8.53	0.27	20.4	6.32	0.31
0.5	44.3	15.06	0.34	30.6	8.56	0.28
0.75	54.8	18.08	0.33	43.7	12.23	0.28
1	69.4	20.12	0.29	63.6	19.08	0.30

Table 6 Stochastic responses of the maximum lateral deflections of pile group with the input COV of 10%

COV = 10% Q/V	Front pile			Rear pile		
	Mean	SD	COV	Mean	SD	COV
0.25	7.5	0.70	0.09	6.4	0.85	0.13
0.5	8.4	0.93	0.11	7.9	1.18	0.15
0.75	9.1	1.39	0.15	8.9	1.26	0.14
1	10.5	2.14	0.20	10.1	1.34	0.13

Table 7 Stochastic responses of the maximum lateral deflections of pile group with the input COV of 20%

COV = 20% Q/V	Front pile			Rear pile		
	Mean	SD	COV	Mean	SD	COV
0.25	7.1	0.97	0.14	6.2	0.98	0.16
0.5	7.9	1.81	0.23	7.6	1.64	0.22
0.75	8.8	1.72	0.20	8.6	1.71	0.20
1	10.3	2.16	0.21	9.8	2.35	0.24

Table 8 Stochastic responses of the maximum lateral deflections of pile group with the input COV of 30%

COV = 30% Q/V	Front pile			Rear pile		
	Mean	SD	COV	Mean	SD	COV
0.25	6.7	1.54	0.23	6.0	1.54	0.26
0.5	7.4	2.14	0.29	7.5	1.74	0.23
0.75	8.6	2.41	0.28	8.4	1.95	0.23
1	10.0	3.10	0.31	9.6	2.78	0.29

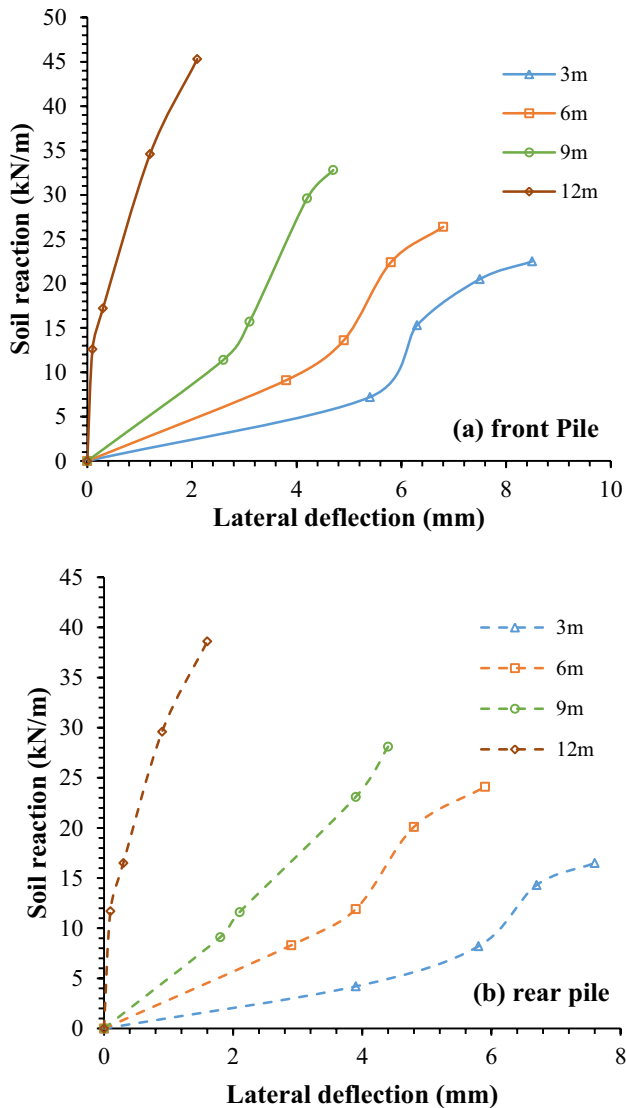


Fig. 19 p - y curves for the pile group **a** front pile **b** rear pile

are higher in the front pile than the rear pile. The stochastic responses for the various depths of the pile are shown in Fig. 20. With regard to the stochastic responses of p - y curves, it is observed that the magnitudes of the soil reaction responses are higher in the case of front piles when compared to the rear piles as also seen in the conventional deterministic cases.

Conclusions

In the present study, the combined action of axial and lateral load on the pile group, with the purpose of including the uncertainty of elastic modulus of soil, is exemplified using the numerical modelling in FLAC3D. The random samples of elastic modulus of soil are adopted to address the parameter uncertainty in the system. A 2×2 pile group embedded in the homogenous cohesionless soil deposit is validated with the existing study and the model is analysed for the combined axial and lateral loading acting on the pile group. The parameter uncertainty in the study is analysed with the inclusion of statistic lognormal distribution of soil's elastic modulus, derived for three different COVs i.e., 10%, 20% and 30% and different Q/V load combinations totally mounting to 12000 Monte Carlo runs and corresponding stochastic behaviours are illustrated.

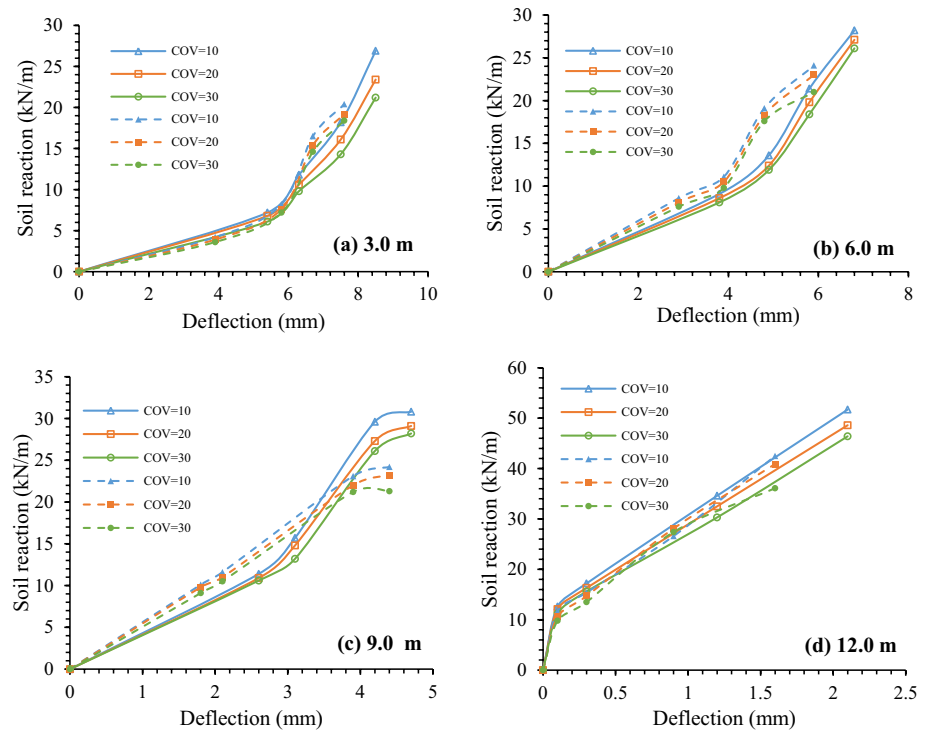
The following observations can be made with regard to the lateral deflection and the bending moment behaviour of all the cases combinedly as:

- The stochastic responses show the significant effect of input COV on all the responses of maximum bending moments and maximum lateral deflections.
- The cdf illustrations plotted for all the Q/V combinations reveal the probability of occurrence of the concerned responses with respect to the input COV. The magnitudes of the variations are also presented for the maximum bending moments and maximum lateral deflections.
- The more scattered responses and thereby the higher magnitudes of standard deviations are observed in the case COV of 30% due to its variation range and it reflects the behaviour of the soil-pile system accordingly.
- In terms of the maximum bending moments, the highest COV across all the responses is found to be as 34% for the Q/V of 0.5, with the input COV of 30%.
- With respect to the maximum lateral deflections, the maximum COV for all the responses is determined to be 31% for the Q/V of 1.0, given an input COV of 30%.

The following findings can be drawn with regard to the soil-reaction incurred due to the application of lateral load of all the cases as:

- The probability distributions of the soil reaction i.e., p - y curves at different locations of the pile along its depth are varying and the probability density fit function fit is complex to illustrate them.

Fig. 20 p - y curves for the front and rear piles for different COVs



- As per the variation in COV, the determined soil-reactions are proportionally scattered and it is sensible to the pile location in its group behaviour.

Overall, the present parameter uncertainty analysis encompasses the necessity of its utilization in determining the soil-pile behaviour when applied with the static axial and lateral loads. The parameter uncertainty in the considered soil property i.e., the elastic modulus of the soil is important in analysing the pile group behaviour, while the uncertainty pertaining to the other soil and pile properties such as density and Poisson's ratio, Young's modulus of pile is less considered in practical cases and so in the present study. The uncertainty pertaining to the soil shear strength parameter i.e., the cohesion c , and the friction angle ϕ based on the soil type can be studied further. The conclusions provided in the above stochastic study may reflect the general validity. Thus, the detailed analysis with the inclusion of all the parameter and model uncertainties altogether is necessary for the safer design of the pile foundations.

Future Scope of the Study

This study focuses on the uncertainty pertaining to the soil's elastic modulus, whereas few other parameters such as the cohesion and the friction angle also carry the uncertainty. The inclusion of other parameter uncertainties imposes higher numerical cost. The limitation can

be addressed using the concept of random field—spatial variability of the parameters along with the scale of fluctuations in the horizontal and vertical directions for all the parameters accordingly for more realistic investigation. The other major limitation in the present study is in regard to the stochastic analysis in the p - y curves. Since the soil reaction profiles are generated at a particular depth of the pile, the resulting distribution and the statistical characterization of the responses become complex for the depiction and it can also be considered for the future studies utilizing the random field implementation.

Authors Contribution SK: Conceptualization, methodology, validation, formal analysis, writing—original draft. KC: conceptualization, methodology, writing—original draft.

Conflict of interest The authors declare that they have no known competing financial interests or personal relationships that could have appeared to influence the work reported in this paper.

References

1. Brown DA, Morrison C, Reese LC (1988) Lateral load behavior of pile group in sand. *J Geotech Eng* 114(11):1261–1276
2. Rollins KM, Lane JD, Gerber TM (2005) Measured and computed lateral response of a pile group in sand. *J Geotech Geoenviron Eng* 131(1):103–114

3. Matlock H, Reese LC (1960) Generalized solutions for laterally loaded piles. *J Soil Mech Found Eng* 86(SM5):63–91
4. Muqtadir A, Desai CS (1986) Three-dimensional analysis of a pile-group foundation. *Int J Numer Anal Methods Geomech* 10(1):41–58
5. Randolph MF, Wroth CP (1978) Analysis and deformation of vertically loaded piles. *J Geotech Eng Div* 104(12):1465–1488
6. Kimura M, Adachi T, Kamei H, Zhang F (1995) 3-D finite element analyses of the ultimate behaviour of laterally loaded cast-in-place concrete piles. In: *Proceedings of the 5th international symposium on numerical models in geomechanics*, 589–594
7. Hussien MN, Tobita T, Iai S, Rollins KM (2010) Soil-pile separation effect on the performance of a pile group under static and dynamic lateral load. *Can Geotech J* 47(11):1234–1246
8. Hazzar L, Karray M, Bouassida M, Hussien MN (2013) Ultimate lateral resistance of piles in cohesive soil. *Deep Found Inst J* 7(1):59–68
9. Hazzar L, Hussien MN, Karray M (2017) On the behaviour of pile groups under combined lateral and vertical loading. *Ocean Eng* 131:174–185
10. Anagnostopoulos C, Georgiadis M (1983) Interaction of vertical and lateral pile responses. *J Geotech Eng Div* 119(4):793–798
11. Achmus M, Thieken K (2010) On the behaviour of piles in non-cohesive soil under combined horizontal and vertical loading. *Acta Geotech* 5(3):199–210
12. Karthigeyan S, Ramakrishna VVGST, Rajagopal K (2006) Influence of vertical load on the lateral response of piles in sand. *Comput Geotech* 33(2):121–131
13. Hussien MN, Tobita T, Iai S, Rollins KM (2012) Vertical load effect on the lateral pile group resistance in sand response. *Int J Geomech Geoeng* 7(4):263–282
14. Hussien MN, Tobita T, Iai S, Karray M (2014) On the influence of vertical loads on the lateral response of pile foundation. *Comput Geotech* 55:392–403
15. Hazzar L, Hussien MN, Karray M (2016) Investigation of the influence of vertical loads on the lateral response of pile foundations in sand and clay soils. *J Rock Mech Geotech Eng* 9(2):291–304
16. Baecher GB, Christian JT (2005) *Reliability and statistics in geotechnical engineering*. Wiley
17. Phoon KK, Kulhawy FH (1999) Characterization of geotechnical variability. *Can Geotech J* 36:612–624
18. Phoon KK, Kulhawy FH (1999) Evaluation of geotechnical property variability. *Can Geotech J* 36:625–639
19. Lacasse S, Nadim F (1996) Uncertainties in characterizing soil properties – plenary paper. In: *Proceedings of ASCE special technical publication No. 58: uncertainty in the geologic environment – from theory to practice*. Madison, Wisconsin, USA. 1, 49–75
20. Lacasse S, Goulois A (1989) Uncertainty in API parameters for predictions of axial capacity of driven pile in sand. In: *Proceedings of 21st OTC*, Houston, Texas, USA. 353–358
21. Halder S, Babu GLS (2008) Effect of soil spatial variability on the response of laterally loaded pile in undrained clay. *Comput Geotech* 35(4):537–547
22. Naghibi F, Fenton GA, Griffiths DV (2016) Probabilistic considerations for the design of deep foundations against excessive differential settlement. *Can Geotech J* 53(7):1167–1175
23. Harmouni A, Dias D, Sbartai B (2017) Probabilistic analysis of piled earth platform under concrete floor slab. *Soils Found* 57(5):828–839
24. Leung YF, Lo MK (2018) Probabilistic assessment of pile group response considering superstructure stiffness and three-dimensional soil spatial variability. *Comput Geotech* 103:193–200
25. Halder K, Chakraborty D (2020) Influence of soil spatial variability on the response of strip footing on geocell reinforced slope. *Comput Geotech* 122:103533
26. Hamrouni A, Badreddine S, Dias, D. (2021) Ultimate dynamic bearing capacity of shallow strip foundations – Reliability analysis using the response surface methodology. *Soil Dyn Earthq Eng* 144(2021):106690
27. Minnucci L, Morici M, Carbonari S, Dezi F, Gara F, Leoni G (2022) Correction to: a probabilistic investigation on the dynamic behaviour of pile foundations in homogeneous soils. *Bull Earthquake Eng* 20(7):3621
28. Song H, Pei H, Zhang P (2023) Probabilistic method for the size design of energy piles considering the uncertainty in soil parameters. *Undergr Space* 10:37–54
29. Kotra S, Chatterjee K (2023) Effect of spatial variability of cone penetration resistance on probabilistic axial capacity of pile foundations. *Mar Georesour Geotechnol*. <https://doi.org/10.1080/1064119X.2023.2280989>
30. Kotra S, Chatterjee K (2023) Static response of a pile group in the domain of uncertainty. In: *Proceedings of geo-congress 2023: foundations, retaining structures, and geosynthetics, geotechnical special publication (GSP) No. 341*, ASCE, Reston, VA, USA, pp 45–53, <https://doi.org/10.1061/9780784484685.005>
31. Itasca, (2017) User's and theory manuals of FLAC3D: fast lagrangian analysis of continua in 3D, version 6. ITASCA Consulting Group Inc., Minneapolis
32. Chatterjee K, Choudhury D, Rao VD, Poulos HG (2019) Seismic response of single piles in liquefiable soil considering P-delta effect. *Bull Earthquake Eng* 17(6):2935–2961
33. Chatterjee K, Choudhury D, Kumar M (2022) Influence of depth of liquefiable soil layer on dynamic response of pile group subjected to vertical load. *Bull Earthquake Eng* 20:113–114
34. Timoshenko SP, Goodier JN (2002) *Theory of elasticity*, 3rd edn. Tata McGraw-Hill Education, New Delhi
35. Al-Shamary JA, Chik Z, Taha MR (2018) Modeling the lateral response of pile groups in cohesionless and cohesive soils. *Geo-Engineering*, 9(1)
36. IS 2911 Part1: Section 4 (2010) Indian standard code of practice for design and construction of pile foundations. Bureau of Indian Standards, New Delhi
37. Paice GM, Griffiths DV, Fenton GA (1996) Finite element modeling of settlements on spatially random soil. *J Geotech Eng* 122(9):777–779
38. Phoon KK, Kulhawy FH (2003) Evaluation of model uncertainties for reliability-based foundation design. In: *Proceedings of 9th international conference on applications of statistics and probability in civil engineering*, San Francisco, USA. July 6–9, 2,1351–135
39. Bowles JE (2012) *Foundation analysis and design*, 5th edn. McGraw-Hill Inc, New York

Publisher's Note Springer Nature remains neutral with regard to jurisdictional claims in published maps and institutional affiliations.

Springer Nature or its licensor (e.g. a society or other partner) holds exclusive rights to this article under a publishing agreement with the author(s) or other rightsholder(s); author self-archiving of the accepted manuscript version of this article is solely governed by the terms of such publishing agreement and applicable law.